

Controller Design for Hypersonic Vehicles Accommodating Nonlinear State and Control Constraints

S. S. Vaddi¹ and P. Sengupta.²

Optimal Synthesis Inc, Los Altos, CA, 94022

A controller formulation suitable for trajectory tracking of a hypersonic vehicle is derived in this paper. The formulation explicitly accommodates nonlinear constraints involving both state and control variables. The controller is demonstrated in closed loop simulations based on an existing longitudinal hypersonic vehicle model. The controller not only successfully tracks the reference trajectories but is also shown to satisfy inequality constraints on variables such as combustor temperature, combustor pressure, engine mass flow rate, and vehicle tip displacement.

Nomenclature

V	=	Velocity
h	=	Altitude
q	=	Pitch attitude rate
θ	=	Pitch attitude angle
α	=	Angle of attack
η_i	=	Generalized flexible body displacements
ω	=	Natural frequency of flexible body modes
ζ	=	Damping associated with flexible body modes
M	=	Mach number

¹ Research Scientist, 95 First Street, Suite 240, Los Altos, CA, AIAA Member.

² Research Scientist, 95 First Street, Suite 240, Los Altos, CA, AIAA Member.

p	=	Pressure
T	=	Temperature
Φ	=	Air-fuel equivalence ratio
δ_{el}	=	Elevator deflection
δ_{ca}	=	Canard deflection
δ_{cd}	=	Cowl door position
A_d	=	Diffuser area ratio
D	=	Aerodynamic drag
L	=	Aerodynamic lift
T	=	Propulsion thrust
A_c, B_c	=	Continuous time system matrices
A, B	=	Discretized system matrices
Q, R	=	State and control weighting matrices
x	=	State vector
f	=	Nonlinear system dynamics vector
u	=	Control vector

I. Introduction

Hypersonic vehicle research and development has been pursued by NASA and different agencies of the DoD repeatedly for the past fifty years [1]-[7]. These vehicles are expected to serve different purposes such as a reusable launch vehicle, rapidly deployable missiles, and Mars entry vehicles. Flight control system design for hypersonic vehicles with air-breathing scramjet engines is more challenging than their subsonic and supersonic counterparts. Some of the challenges are:

- (i) Wide range of couplings between aerodynamic, structural, thermal, and propulsion models.
- (ii) Modeling uncertainties.
- (iii) State & control constraints reflecting the fragile conditions under which the vehicle can operate.

Some of the past modeling efforts include the model by Chavez and Schmidt [7] which is a longitudinal dynamic model. Newtonian impact theory is used for computing the aerodynamic forces in this work. The model includes aero-structural and aero-propulsive couplings. Recent models [8]-[11] by Mirmirani et.al are based on CFD and FEM modeling. Both longitudinal and six degree of freedom models have been developed in these papers. Longitudinal models have been developed by Bolender et.al in [12]-[15]. These models are extensions of Chavez and Schmidt's model. Oblique shock theory and Prandtl Meyer expansion theory are used to compute aerodynamic normal pressure distribution. Structural model in [13] uses two cantilever beams fixed at the center. The model in [13] has an inertial structural coupling which is eliminated in [15]. Assumed modes method is used in [14]-[15] for modeling the structural dynamics. Also included in [15] are viscous and unsteady aerodynamic effects and thermo-elastic interactions. An exhaustive description of the challenges and trends in the modeling and control of scramjet-powered hypersonic vehicles is given in [16].

Guidance and integrated control issues of hypersonic vehicles have been addressed in [17]-[20]. A significant portion of the research in controller design for hypersonic vehicles [21]-[30] has focused on adaptive and robust control formulations. These works address the uncertainties in the hypersonic vehicle models used for controller design. Some of the other works such as [31] involves development of conventional auto-pilot design. A linear parameter varying model is used for controller design [32] and differential algebraic approach is used in [33].

Hypersonic vehicles operate under much more fragile conditions and are prone to phenomena such as thermal choking [16], flow disassociation, ionization. As advanced research further unravels these phenomena it is expected that these conditions can be represented as constraints on variables such as Mach numbers, pressures and temperatures at different locations of the hypersonic vehicle. Safety and performance restrictions on temperatures and displacements of sensor locations can also be translated into constraints on state and control variables. The objective of the current research is to develop a controller design that can accommodate nonlinear state and control constraints. In addition to implementing safety features these constraints also facilitate inclusion of explicit closed loop performance specifications in the design process. A model predictive controller (MPC) framework is employed for this purpose. It should be noted model predictive control offers the most promising methodology for handling state and control constraints. Moreover the approach is completely numerical therefore scalable for higher dimensional system. Model predictive control approaches have been used successfully in the past for different [34]-[36] aerospace engineering control problems such as spacecraft formation flying, moving mass actuated missile

control, and control of an F-16 aircraft. Another attractive feature of MPC is that they do not require explicit analytic models. Hypersonic vehicle models generated using computational techniques such as CFD and FEM are unlikely to have an analytic representation. MPC is widely used in industry for slowly varying dynamic systems and is implemented at low update rates. However, advances in convex optimization research such as [37] make it possible to implement these controllers for fast-varying dynamical systems such as a hypersonic vehicle, in real-time, at very high update rates.

Briefly described in Section II is the hypersonic vehicle model used in this research. The model is based on the work of Bolender et. al [12]-[15] and is widely used in recent literature. A discretized version of the model suitable for MPC formulation is derived in Section III. Model predictive formulation accommodating nonlinear constraints is derived in Section IV. Closed loop simulation results are presented in Section V.

II. Hypersonic Vehicle Model

The equations of motion for a hypersonic vehicle can be written as $\dot{x} = f(x, u)$ which is expanded below [14]:

$$\begin{aligned}
 \dot{V} &= (T \cos \alpha - D)/m - g \sin \gamma \\
 \dot{\alpha} &= -(T \sin \alpha + L)/(mV) + (g/V - V/r) \cos \gamma + q \\
 \dot{q} &= M_p / I_{yy} \\
 \dot{\theta} &= q \\
 \dot{h} &= V \sin \gamma \\
 \ddot{\eta}_i &= -2\zeta\omega_i\dot{\eta}_i - \omega_i^2\eta_i + G_i, i = 1..3
 \end{aligned} \tag{1}$$

where the state vector is $x = [V \ \alpha \ q \ \theta \ h \ \eta_1 \ \dot{\eta}_1 \ \eta_2 \ \dot{\eta}_2 \ \eta_3 \ \dot{\eta}_3]$ and the control vector is represented by $u = [\Phi \ \delta_{el} \ \delta_{ca} \ A_d \ \delta_{cd}]$. The control vector consists of fuel-equivalence ratio, elevator deflection, canard deflection, diffuser area ratio, and the cowl door position. In this work only the first two controls are used. Computation of the aerodynamic forces and moments along with propulsion thrust is computed based on [12]-[15]. In this work it is assumed that these forces and moments are computed as a function $F(x, u)$ of the state and control vectors by a computer program. Explicit analytical use of the right hand side of Eq. (1) is not made anywhere in the controller design.

$$[L \ D \ T \ M_p \ G_i] = F(x, u) \tag{2}$$

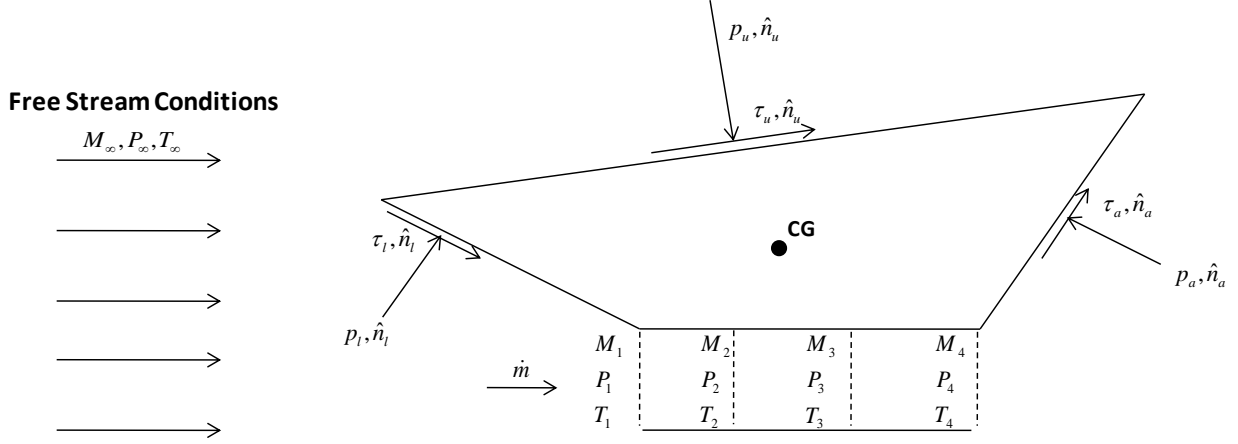


Figure 1. Schematic of a Hypersonic Vehicle with Air-Breathing SCRAMJET Engine

As mentioned earlier apart from the state components such as velocity, altitude and angle-of-attack it is also of interest to compute and control variables such as Mach numbers and temperatures at various locations of the hypersonic vehicle as shown in Figure 1. Computation of these variables is essential for the computation of forces and moments, therefore, it is assumed in this work that these variables are also obtained from a computer program as a function $z(x, u)$ of the state and control vectors.

$$\left[M_1 \quad p_1 \quad T_1 \quad M_2 \quad p_2 \quad T_2 \quad \dots \quad \dot{m} \quad \Delta_{tip} \right] = z(x, u) \quad (3)$$

III. Discretization

Model predictive controller formulations are inherently discrete-time formulations. Therefore, the first step in designing a model predictive controller involves discretization of the nonlinear dynamic system. Equations of motion described in the previous chapter constitute the nonlinear system description in the following equation:

$$\dot{x} = f(x, u) \quad (4)$$

Next step involves linearization of these equations about a trim condition which is an equilibrium point for the dynamic system.

$$x^*, u^* \text{ Equilibrium Point} \Rightarrow f(x^*, u^*) = 0$$

Linearized model is described by variables which are deviations from the equilibrium:

$$x = x^* + \delta x \quad u = u^* + \delta u \quad (5)$$

The system matrices A_c and B_c for the linearized model are obtained by taking Jacobians of the nonlinear vector field $f(x,u)$ with respect to x and u :

$$\delta\dot{x} = \frac{\partial f}{\partial x} \delta x + \frac{\partial f}{\partial u} \delta u = A_c \delta x + B_c \delta u \quad (6)$$

Discretized version of the continuous time linear system in the above equation is described by the following equations:

$$\delta x[k+1] = A \delta x[k] + B \delta u[k] \quad (7)$$

Discretization can be done using ‘ZOH’ by the following equations:

$$A = e^{A_c dt} \quad B = \int_0^{dt} e^{A_c s} B_c ds \quad (8)$$

In this work the Jacobians are computed numerically using finite differencing technique and the discretization is done using MATLAB’s ‘c2d’ command.

IV. Model Predictive Controller Formulation

A. Trajectory Tracking

Model predictive controller formulation is essentially an optimization problem with an objective function to be minimized, equality constraints to be satisfied and inequality constraints to be adhered. Shown below is the optimization formulation associated with the model predictive controller formulation:

$$\begin{aligned} \text{minimize } J &= \sum_{k=N_1}^N (\delta x[k] - \delta x_{ref}[k])^T Q (\delta x[k] - \delta x_{ref}[k]) + \sum_{k=1}^{N_2} \delta u^T[k] R \delta u[k] \\ \text{subject to } \delta x[k+1] &= A \delta x[k] + B \delta u[k], k = 1..(N-1) \\ x_{\min} &\leq x^* + \delta x[k] \leq x_{\max}, k = 2..N \\ u_{\min} &\leq u^* + \delta u[k] \leq u_{\max}, k = 1..(N-1) \\ \delta u[N_2 : N] &= \delta u[N_2] \\ \delta x[1] &= x - x^* \end{aligned} \quad (9)$$

Objective function used in this problem involves two cost components. The first component penalizes trajectory departure from the desired reference trajectory and the second component penalizes the controls. Different horizons are used for the trajectory cost component and the control cost component. Control is penalized over a short duration

from the current time instant. This horizon is referred to as cost horizon. It is expected that the effects of control are observed a little later due to the dynamics of the system therefore, trajectory deviations are not penalized in the immediate short duration. The horizon associated with the trajectory deviations is referred to as the prediction horizon. Typically the prediction horizon is much larger than the cost horizon. The control is kept constant for the duration between the cost horizon and the prediction horizon. The discrete-time propagation equation over the prediction horizon is implemented as equality constraints. The desired limits for the state and control are implemented as inequality constraints. The controller design is based on a linear model using variables that represent a departure from the equilibrium. However, the controller is implemented on the actual nonlinear model and the limits are implemented on the actual state and control variables.

B. Nonlinear Output Constraints

While constraints on state and control variables for implementing the desired limits are straightforward to implement, the same cannot be said about constraints on nonlinear output variables such as the following.

$$z = z(x, u) \quad (10)$$

$$z_{\min} \leq z \leq z_{\max} \quad (11)$$

A linearization approach is adopted in the current research to address these constraints as shown below:

$$z \approx z(x^*, u^*) + \frac{\partial z}{\partial x} \delta x + \frac{\partial z}{\partial u} \delta u \quad (12)$$

Partial derivatives with respect to the state and control variables are obtained using finite differencing technique. The constraint is finally implemented in the optimization formulation as a linear constraint on the state and control deviations as shown below:

$$z_{\min} - z(x^*, u^*) \leq \frac{\partial z}{\partial x} \delta x + \frac{\partial z}{\partial u} \delta u \leq z_{\max} - z(x^*, u^*) \quad (13)$$

The above equation can be discretized and added as a linear inequality constraint to the optimization formulation in Eq. (9) for $k=1..N$ as shown below:

$$z_{\min}[k] - z(x^*[k], u^*[k]) \leq \left. \frac{\partial z}{\partial x} \right|_{x^*[k], u^*[k]} \delta x[k] + \left. \frac{\partial z}{\partial u} \right|_{x^*[k], u^*[k]} \delta u[k] \leq z_{\max}[k] - z(x^*[k], u^*[k])$$

C. CVX

CVX (Ref.[38]) is a MATLAB software for formulating and solving convex optimization problems. The software is particularly suitable for rapid prototyping. CVX software has been developed by Michael Grant et. al from Stanford University. The core solvers used in by CVX are SeDuMi and SDPT3. Both these solvers and the CVX software are open source. All optimization problems resulting from the model predictive controller formulations in this research have been solved using this software.

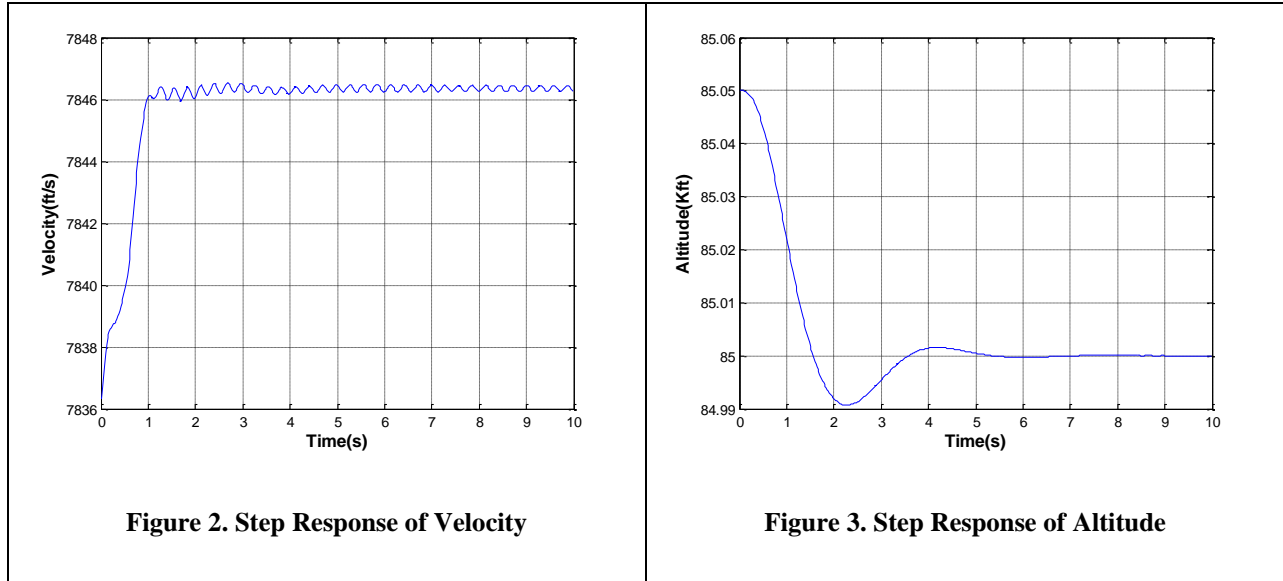
V. Results

The closed loop simulation is done in MATLAB. Equations of motion described in Section II are used for simulation. Model predictive controller design described in section III is implemented using CVX. A sample time of 0.02s is used for discretization. Flight condition corresponding to Mach number of 8.5 and altitude 85000ft is used for linearization. Elevator and the fuel equivalence ratio are used as controls. Step and spline trajectory commands in velocity, altitude and trajectory commands are used for controller testing. The control horizon is set to 5 time steps and the cost horizon is set to 50 time steps starting from 10 time steps. The control limits are set as follows:

$$\begin{aligned} -15^{\circ} &\leq \delta_{elevator} \leq 30^{\circ} \\ 0.1 &\leq \Phi \leq 1.25 \end{aligned} \tag{15}$$

A. Step Response

Shown in Figure 2 and Figure 3 are the step response plots of velocity and altitude. The step command for velocity is 10ft/s and step command for altitude is -50ft.



The Q and R matrices used in this example are:

$$Q = \begin{bmatrix} 1e2 & 0 & 0 & 0 & 0 \\ 0 & 1e4 & 0 & 0 & 0 \\ 0 & 0 & 1e4 & 0 & 0 \\ 0 & 0 & 0 & 1 & 0 \\ 0 & 0 & 0 & 0 & 1e4 \end{bmatrix} \quad R = \begin{bmatrix} 1e4 & 0 \\ 0 & 1e3 \end{bmatrix} \quad (16)$$

The steady state errors in velocity and altitude are 0.1ft/s and 0.05ft. Control time histories are shown in Figure 4 and Figure 5. Saturation is observed in the initial portion of the equivalence ratio time history. Large errors at time $t=0$ typically result in large control magnitudes. The flight path angle time history in Figure 6 is typical of vehicle lowering its altitude and pitch rate time history in Figure 7 indicates stability of the attitude of the vehicle while tracking the step commands.

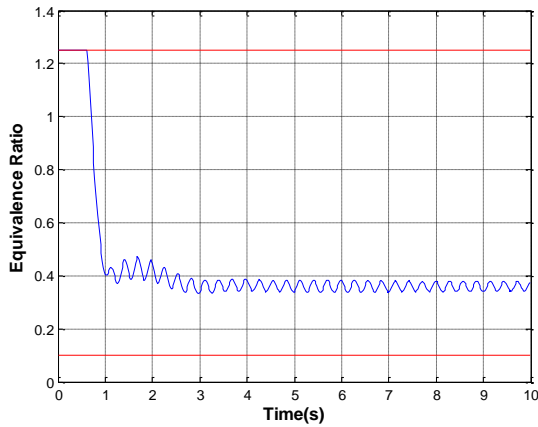


Figure 4. Time History of Equivalence Ratio Control

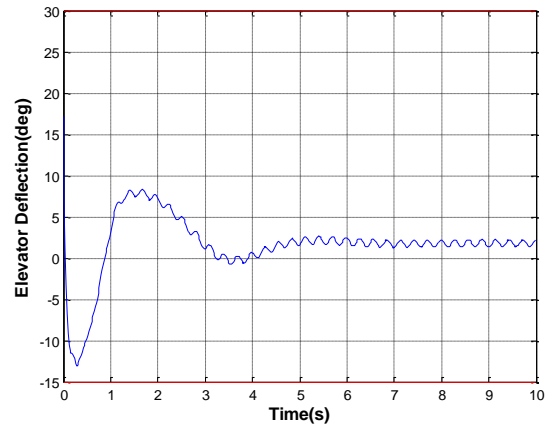


Figure 5. Time History of Elevator Control

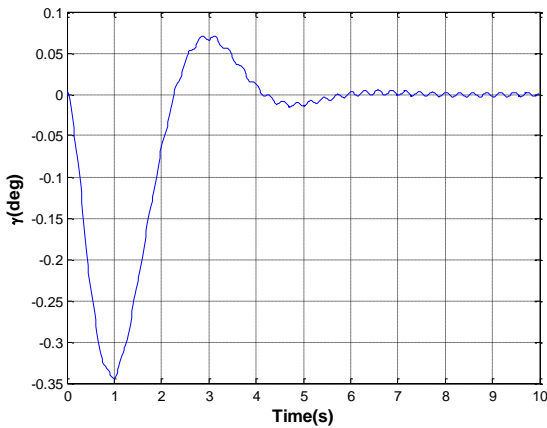


Figure 6. Time History of Flight Path Angle

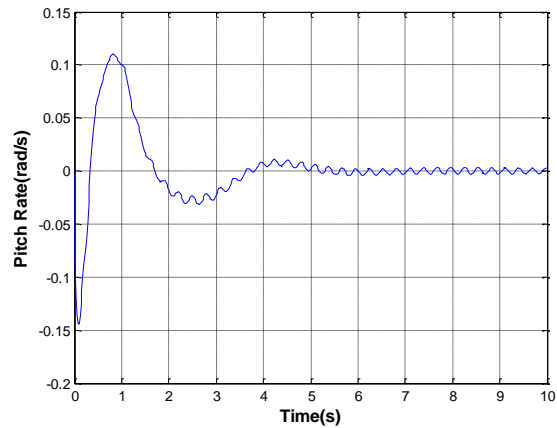


Figure 7. Time History Pitch Rate

Tests have been conducted with positive and negative step commands and in four different combinations.

The closed loop performance is similar in all the tests as shown in Figure 8 and Figure 9. Each of these figures consists of four step response plots of velocity and altitude in different combinations. The four combinations result from the different combinations of positive and negative velocity and altitude steps. The steady state errors in velocity and altitude are 0.1ft/s and 0.05ft in all the four cases.

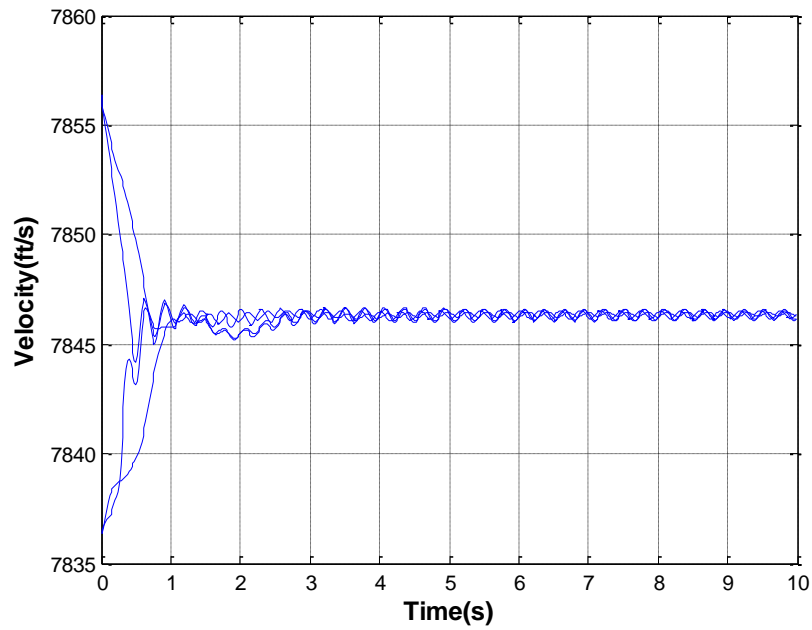


Figure 8. Step Responses to Velocity Commands

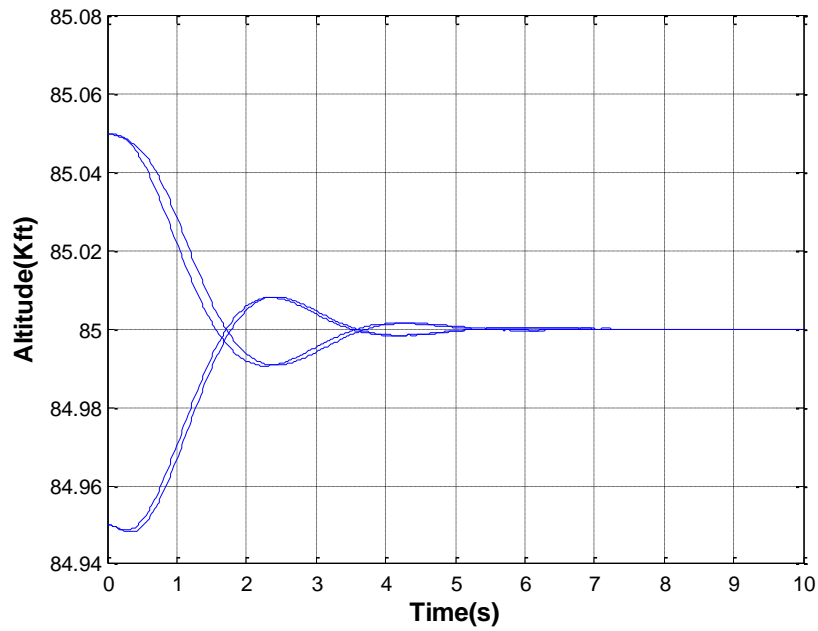
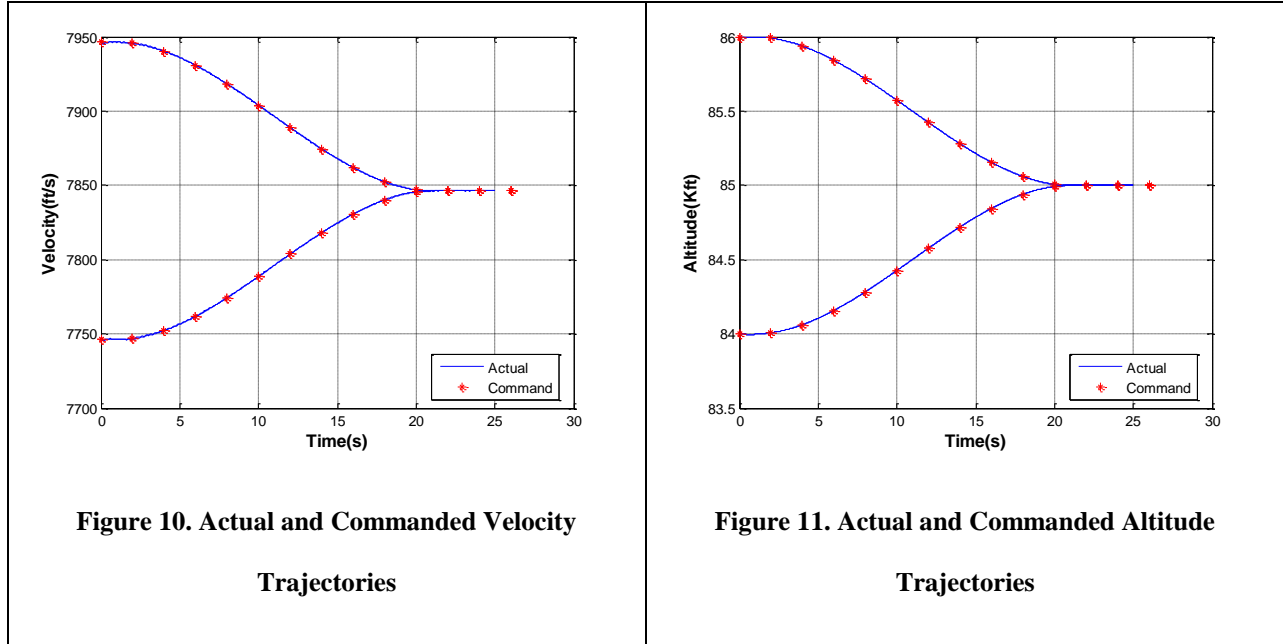


Figure 9. Step Responses to Altitude Commands.

B. Trajectory Tracking

Shown in Figure 10 and Figure 11 are the trajectory tracking performances of the model predictive controller. The trajectories are constructed using a spline fit over 100ft/s change in velocity and 1000ft change in altitude. Commanded and actual trajectories from four different examples involving positive and negative change in velocity together with a positive and negative change in altitude are presented in these figures.



Flexible body modes are not included in the controller design and Q and R matrices are chosen as follows:

$$Q = \text{diag}([1e2 \ 0 \ 0 \ 1 \ 0]) \quad R = \text{diag}([1e4 \ 1e3]) \quad (17)$$

The maximum error in velocity is less than 1ft/s as seen in Figure 12 and the maximum error in altitude tracking is less than 5ft as seen in Figure 13. Control time histories are shown in Figure 14 and Figure 15. The controls are within their limits and no saturation is observed. Flight path angle, pitch attitude angle, angle of attack and pitch attitude rate are shown in Figure 16-Figure 19. The plots in these figures are almost mirror images due to the symmetric nature of the tracking trajectories used.

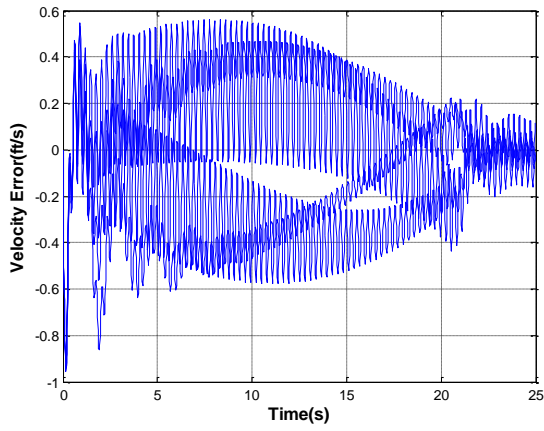


Figure 12. Velocity Tracking Errors

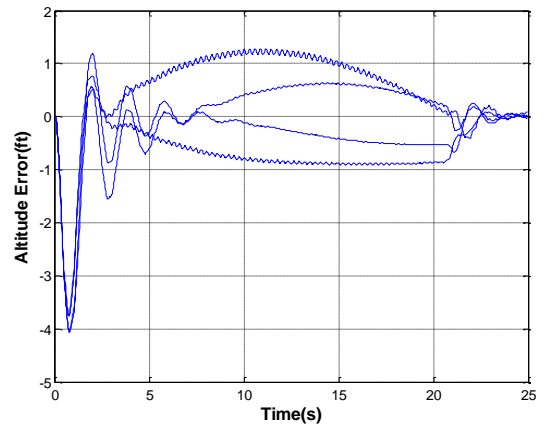


Figure 13. Altitude Tracking Errors

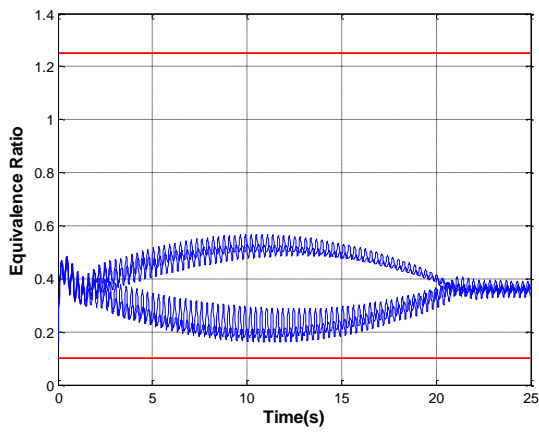


Figure 14. Equivalence Ratio Time Histories

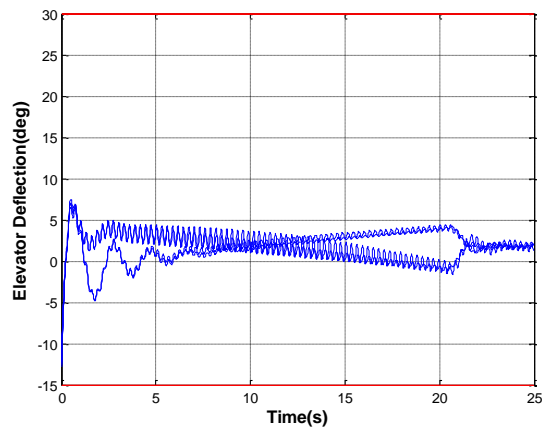
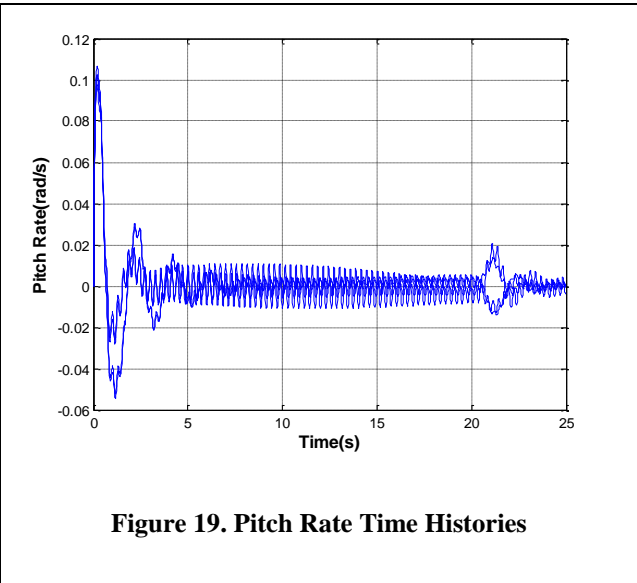
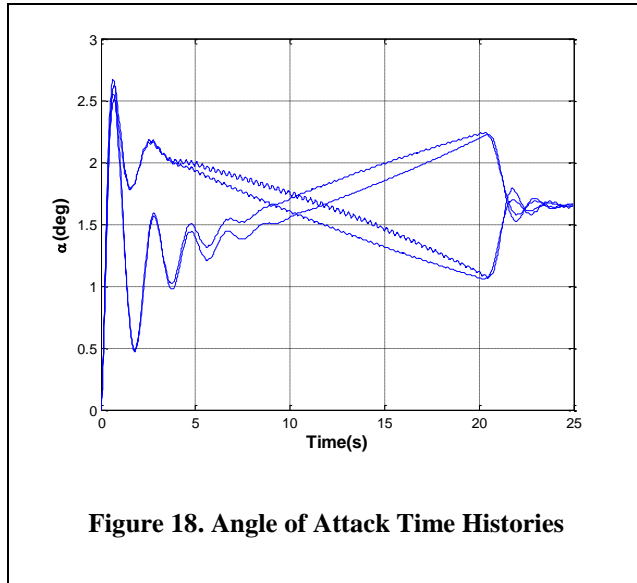
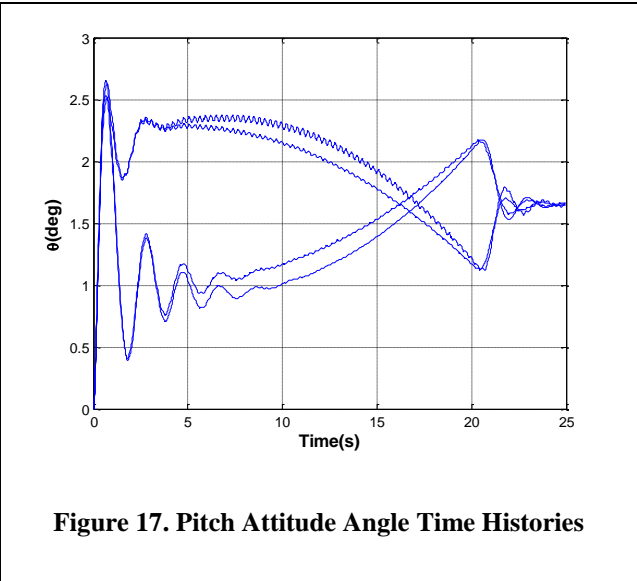
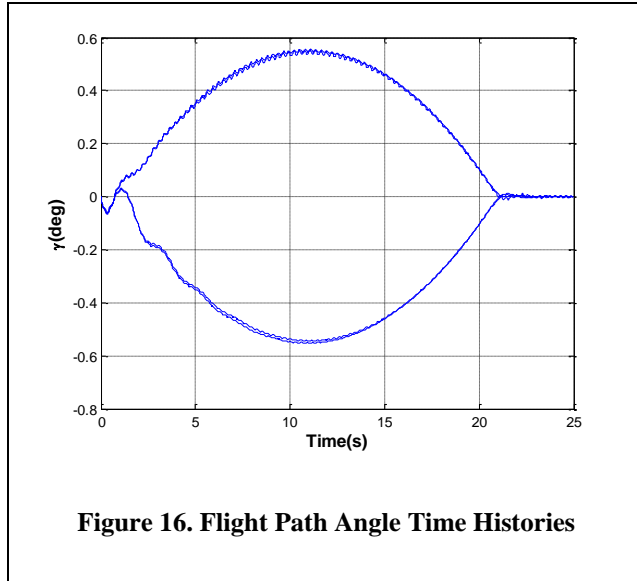


Figure 15. Elevator Deflection Time Histories

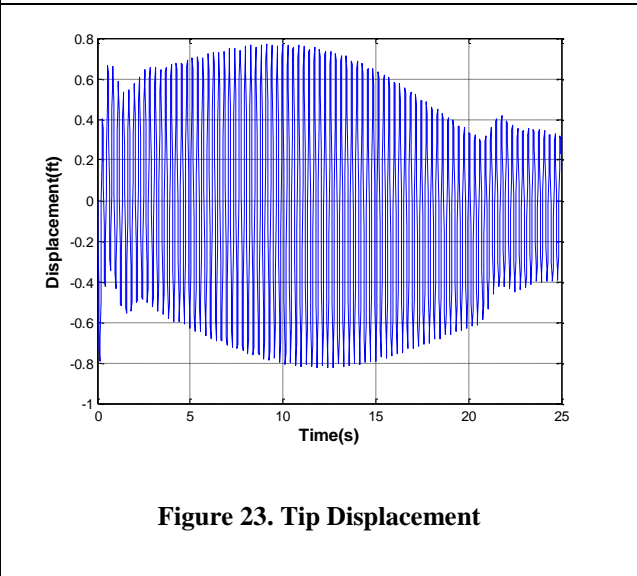
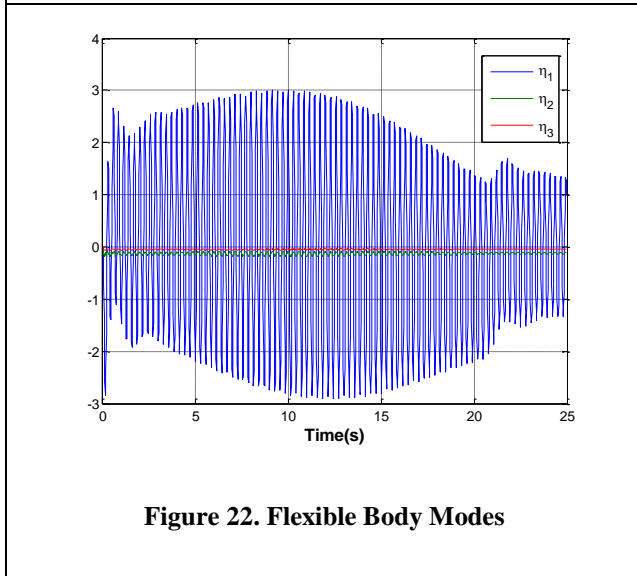
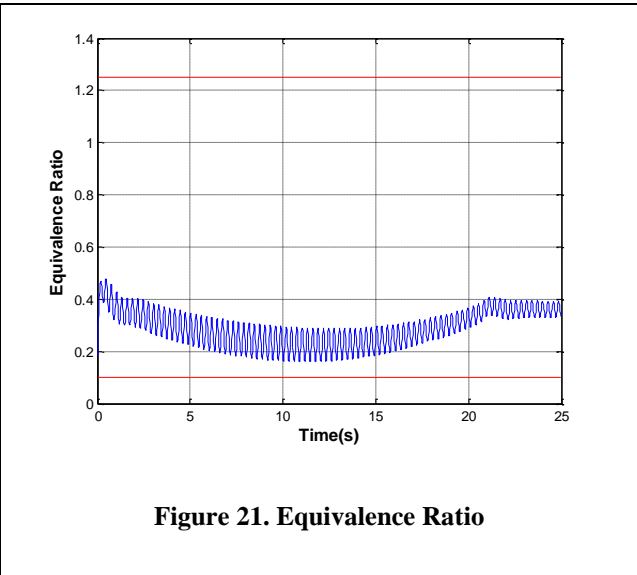
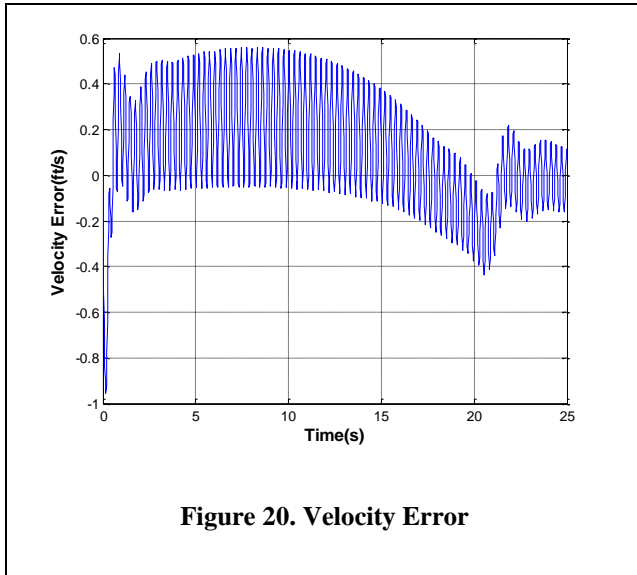


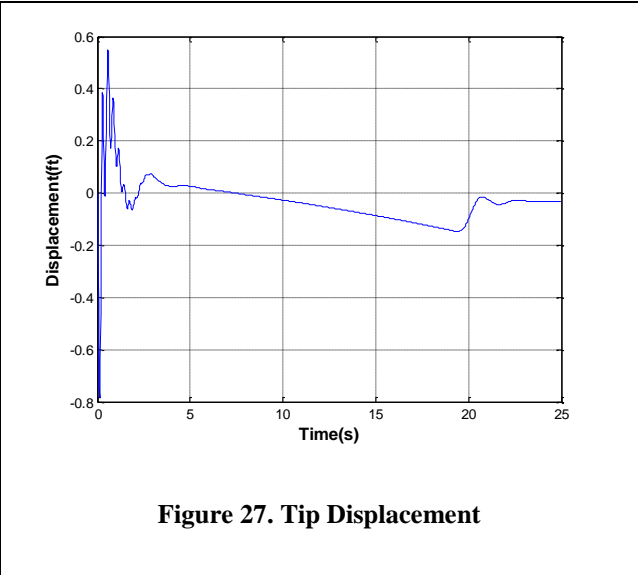
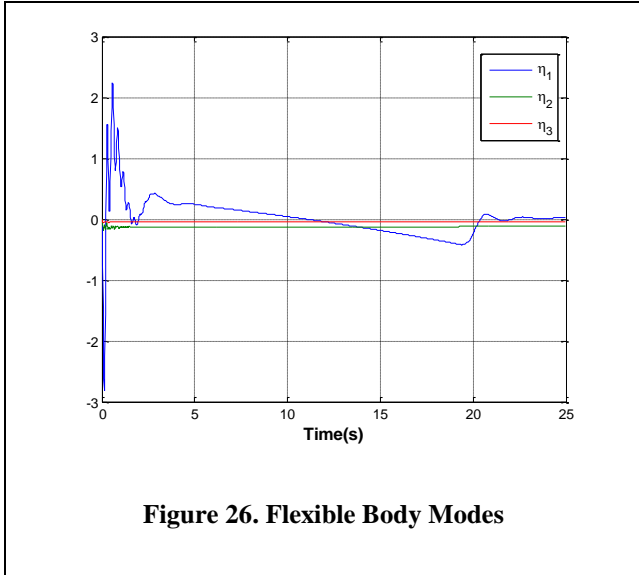
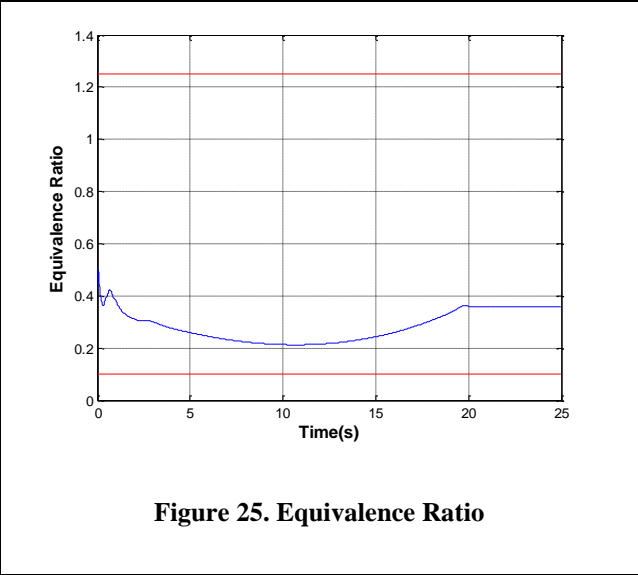
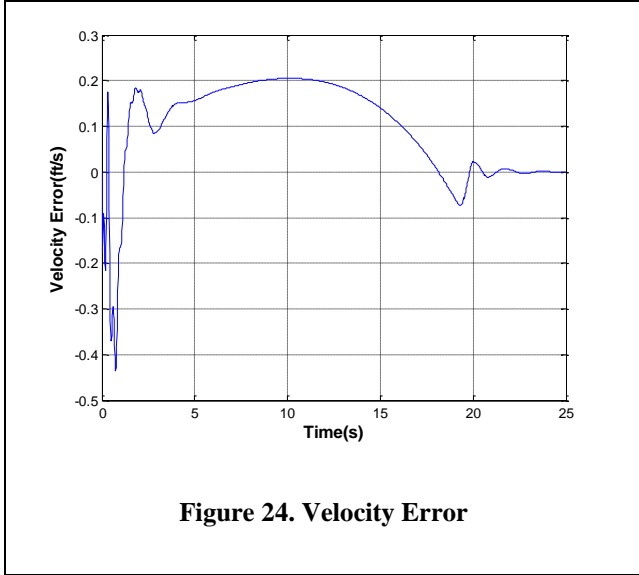
C. With and Without Flexible Body Modes

Controller implemented in the previous sub-section does not include flexible body modes. Therefore, no active mechanism is involved in dampening the vibration. In the current example it is assumed that the flexible body modes are available for feedback and are penalized in the objective function. The Q matrix involves terms from the flexible body modes as well:

$$Q = \text{diag}([100 \ 0 \ 0 \ 1 \ 0 \ 10 \ 0 \ 1 \ 0 \ 1 \ 0]) \quad R = \text{diag}([1e4 \ 1e3]) \quad (18)$$

Shown in Figure 20-Figure 23 are the velocity tracking error, equivalence ratio, flexible body modes and the tip displacement of the vehicle without the flexible body modes in the control design model. A stark contrast exists between these plots and their counterparts in Figure 24-Figure 27 where the high frequency content is completely eliminated.



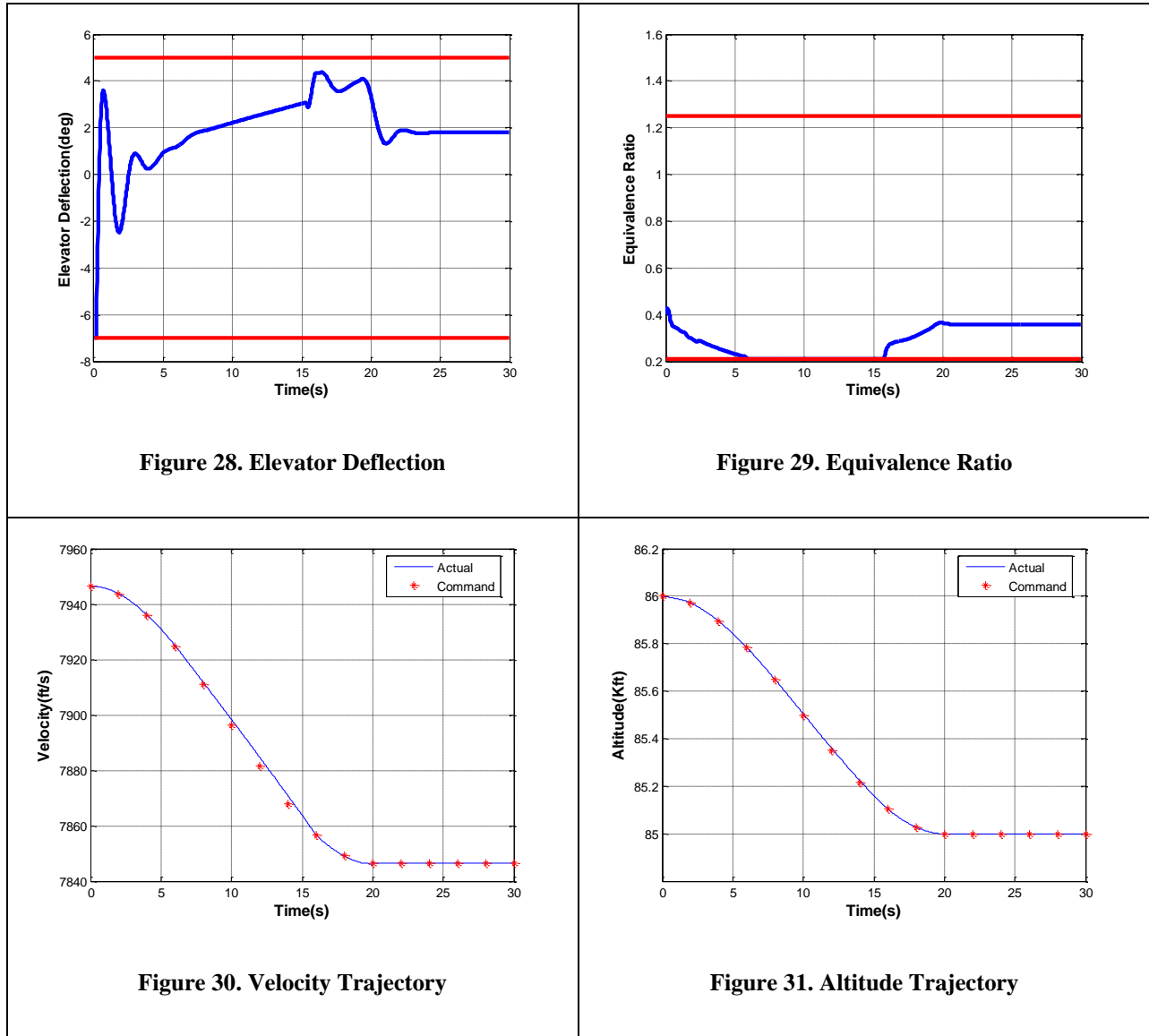


D. Stricter Control Limits

Control time histories in the previous sub-section indicated no saturation. The limits have been deliberately tightened to explore the capability of the model predictive controller in adhering to the limits. The following limits are used in the current example.

$$\begin{aligned}
 -7^\circ &\leq \delta_{elevator} \leq 5^\circ \\
 0.2 &\leq \Phi \leq 1.25
 \end{aligned}
 \tag{19}$$

Shown in Figure 28 and Figure 29 are the control histories for the trajectory tracking example involving negative change in velocity and positive change in altitude. The limits are plotted using thick dark lines. The tracking performance of the controller shown in Figure 30 and Figure 31 only suffers marginally, ending up with a 3.2ft/s maximum error in velocity tracking and 9.4ft maximum error in altitude tracking.

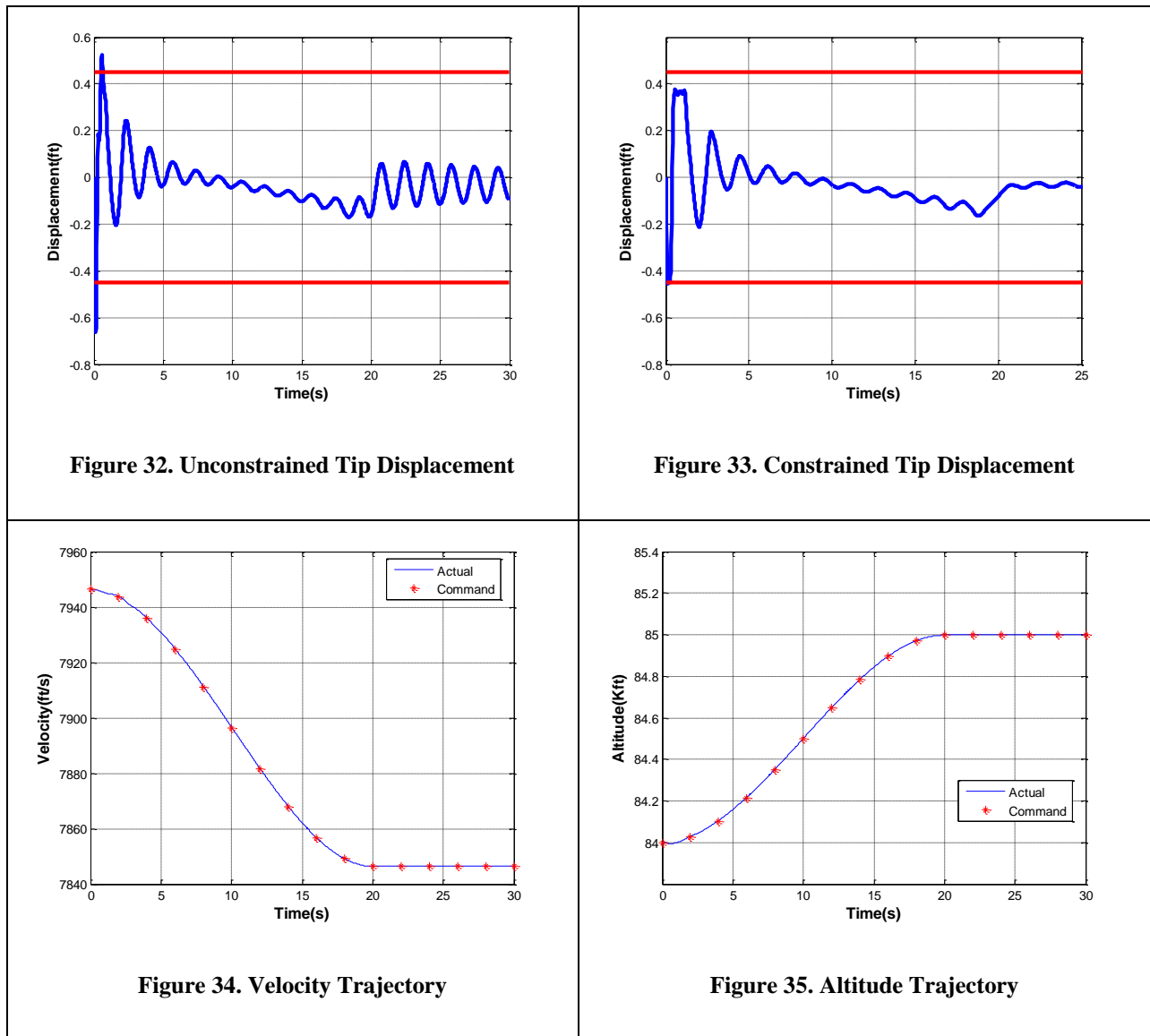


E. Tip Displacement Constraint

The tip displacement of the vehicle is a linear function of the flexible body models alone. It can be written as follows:

$$\Delta_{tip} = \psi_1(0)\eta_1 + \psi_2(0)\eta_2 + \psi_3(0)\eta_3 \quad (20)$$

Where $\psi_i(0)$ is the i^{th} mode shape evaluate at the tip ($L=0$). Unlike the mass flow rate the tip displacement is a linear function of the state variables. Shown in Figure 32 and Figure 33 are the unconstrained and the constrained tip displacement time histories. The sharp peaks at the beginning are eliminated by the constrained model predictive controller. Minor impact has been observed on the trajectory tracking performance shown in Figure 34 and Figure 35 resulting in a maximum velocity tracking error of 0.8ft/s and maximum altitude tracking error of 4.6ft.



F. Mass-Flow Rate Constraint

The mass flow rate through the SCRAMJET inlet is a nonlinear function of the state variables:

$$\dot{m} = \dot{m}(V, h, \alpha, \eta_1, \eta_2, \eta_3) \quad (21)$$

A lower limit on the mass flow rate through the engine is implemented using the approach laid out in section 3.3. Shown in Figure 36 and Figure 37 are the unconstrained and constrained mass flow rate time histories. Although, there is a strong indication of adherence to the constraint the mass flow rate does not exactly achieve the prescribed lower limit. This is due to the fact that only the linearized version of the constraint is actually implemented in the control design model, while the actual simulation uses the full fledged nonlinear model. Minimal effect is noticed on the tracking error due to the introduction of this constraint as seen in Figure 38 and Figure 39. The maximum velocity tracking error is 0.5ft/s and the maximum altitude tracking error is 3.3ft.

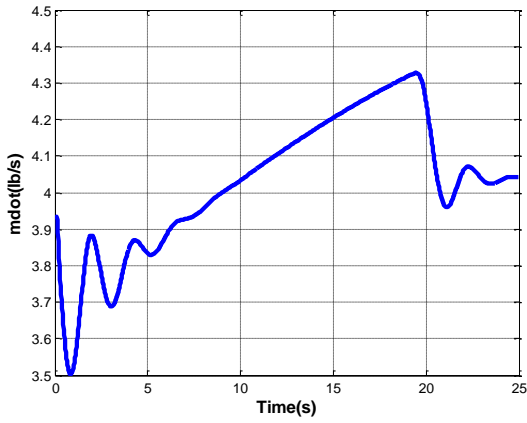


Figure 36. Unconstrained Mass Flow Rate Through the SCRAMJET

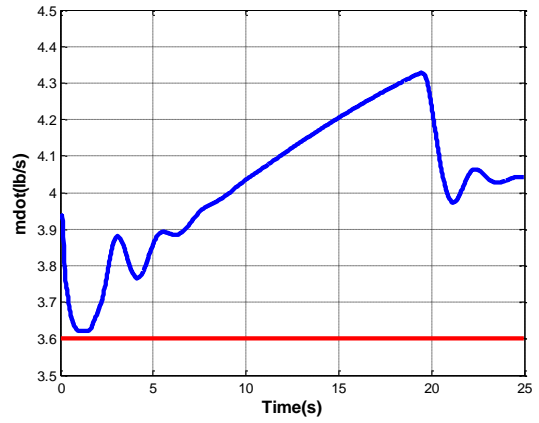


Figure 37. Constrained Mass Flow Rate Through the SCRAMJET

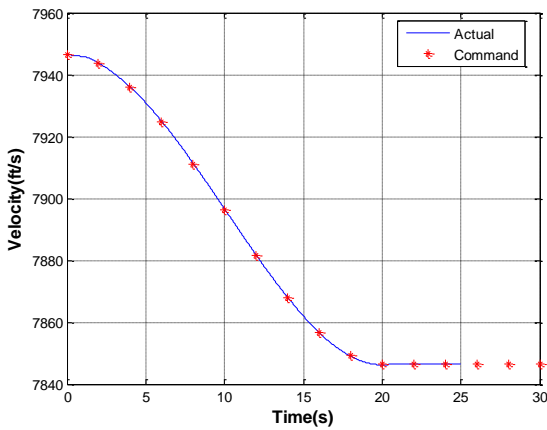


Figure 38. Velocity Trajectory

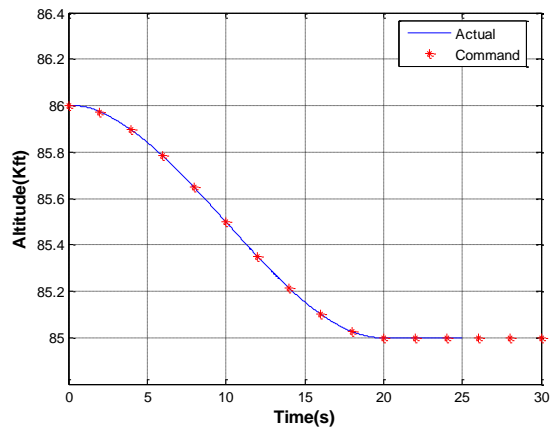


Figure 39. Altitude Trajectory

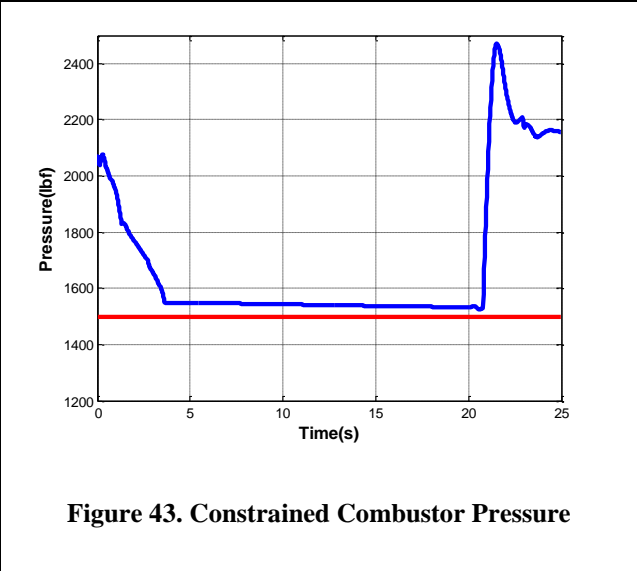
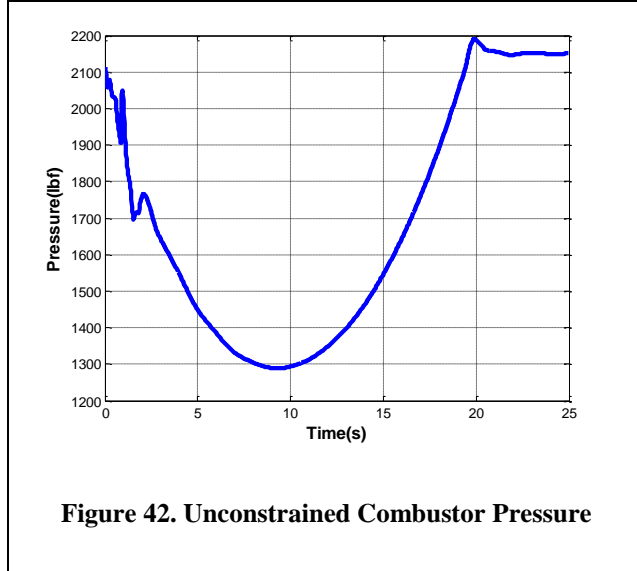
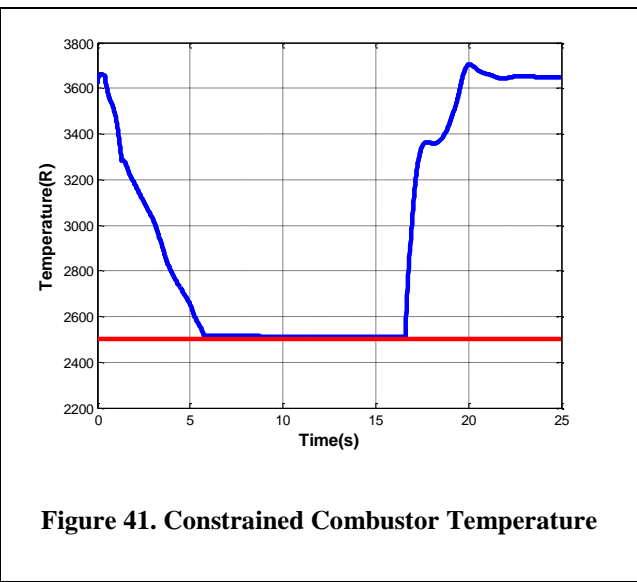
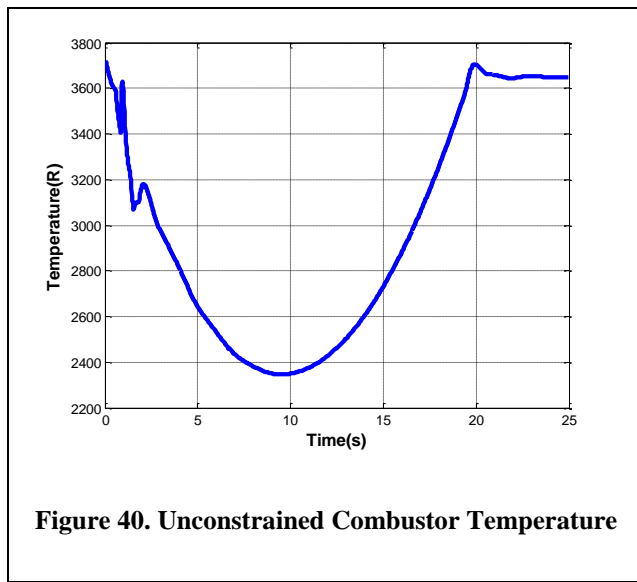
G. SCRAMJET Combustor Temperature and Pressure Constraints

The nonlinear constraint implementation approach has been tested on variables such as combustor pressure (p_3) and temperature (T_3). Unlike the previous variables these two variables are strong functions of the equivalence ratio control variable.

$$p_3 = p_3(V, h, \alpha, \eta_1, \eta_2, \eta_2, \Phi) \quad (22)$$

$$T_3 = T_3(V, h, \alpha, \eta_1, \eta_2, \eta_2, \Phi) \quad (23)$$

Therefore, the resulting constraints involve a combination of both state and control variables. Shown in Figure 40 and Figure 41 are the time histories of the combustor pressure without and with the constraint respectively. Similar plots for pressure are shown in Figure 42 and Figure 43. From the plots there is ample evidence to suggest that the model predictive controller formulation is able to implement constraints on nonlinear output variables. The constraints are not exactly realized in closed loop simulations due to the linearization of the constraints and the implementation on the full nonlinear simulation. Reference trajectories for these two examples are the same those as in Figure 38 and Figure 39. The maximum tracking errors with temperature constraint are 4.6ft/s and 19.6ft. Similar errors with the pressure constraint are 18ft/s and 100ft.



VI. Conclusion

A model predictive controller formulation suitable for trajectory tracking problems is derived in this paper. The formulation explicitly handles control limits and nonlinear constraints involving both state and control variables. The controller is demonstrated in closed loop simulations while keeping within desired limits variables such as combustor temperature, pressure, mass flow rate and tip displacement.

Acknowledgments

The work presented in this paper was sponsored by a phase I SBIR effort from NASA Glenn research center. Authors would like to thank Mike Bolender at AFRL for providing the hypersonic vehicle model and Don Soloway at NASA Ames research center for monitoring this project and providing useful inputs on MPC formulations.

References

- ¹Hallion, R. P., "The History of Hypersonics: or "Back to the Future – Again and Again",” 43rd Aerospace Sciences Meeting and Exhibit, Jan. 2005, Reno, NV, AIAA-2005-0329.
- ²Anon., NASA X-43 Fact Sheet (<http://www.nasa.gov/centers/dryden/news/FactSheets/FS-040-DFRC.html>).
- ³Bradford, J. E., Wallace, J. G., Charania, A. C., and Eklund, D. R., "Quicksat: A Two-Stage to Orbit Reusable Launch Vehicle Utilizing Air-Breathing Propulsion for Responsive Space Access," SPACE 2004 Conference and Exposition, Sep. 2004, San Diego, CA, AIAA-2004-5950.
- ⁴Kokan, T., Olds, J.R., Hutchinson, V., Reeves, J.D., "Aztec: A TSTO Hypersonic Vehicle Concept Utilizing TBCC and HEDM Propulsion Technologies," AIAA 2004-3728, 40th AIAA/ASME/SAE/ASEE Joint Propulsion Conference And Exhibit, 11 - 14 July, 2004, Fort Lauderdale, Florida.
- ⁵Anon., *Aviation Week and Space Technology*, McGraw-Hill Companies, Oct. 29, 1990, p. 40.
- ⁶Bradford, J. E., Olds, J. R., and Wallace, J. G., "A Two-Stage Spacelift Concept Using Air-Breathing Propulsion and Falcon-Derived Hardware," 54th Joint Army-Navy-NASA-Air Force (JANNAF) Propulsion Meeting (JPM) and 5th Modeling and Simulation / 3rd Liquid Propulsion / 2nd Spacecraft Propulsion Joint Subcommittee Meeting, Denver, Colorado, May 14-18, 2007.
- ⁷Chavez, F. R., and Schmidt D. K., "Analytical Aeropropulsive/Aeroelastic Hypersonic-Vehicle Model with Dynamic Analysis," *Journal of Guidance, Control, and Dynamics*, Vol. 17, No. 6, November-December, 1994.

- ⁸Clark, A. D., Mirmirani D., Wu C., and Choi, S., "An Aero-Propulsion Integrated Elastic Model of a Generic Airbreathing Hypersonic Vehicle," AIAA Guidance, Navigation and Control Conference, August 2006, Keystone, CO, AIAA-2006-6560.
- ⁹Clark, A., Wu, C., Mirmirani, M., Choi, S., "Development of an Airframe Integrated Generic Hypersonic Vehicle Model," AIAA Aerospace Conference and Exhibit, Reno, Nevada, January 2006
- ¹⁰Keshmiri, S., Colgren, R., and Mirmirani, M., "Six-DOF Modeling and Simulation of a Generic Hypersonic Vehicle for Control and Navigation Purposes," AIAA Guidance, Navigation, and Control Conference and Exhibit, 2006, Keystone, Colorado
- ¹¹Keshmiri, S., Colgren, R., and Mirmirani, M., "Six-DOF Nonlinear Equations of Motion for a Generic Hypersonic Vehicle for Control and Navigation Purposes," AIAA Atmospheric Flight Mechanics Conference and Exhibit, 2007, Hilton Head, South Carolina
- ¹²Doman, D. B., "Modeling and Control Challenges for Airbreathing Hypersonic Vehicles," SAE Aerospace Guidance and Control Systems Committee Meeting, Boulder, CO, February 28 - March 2, 2007.
- ¹³Bolender, M. A., and Doman, D. B., "Nonlinear Longitudinal Dynamical Model of an Air-Breathing Hypersonic Vehicle," Journal of Spacecraft and Rockets, Vol. 44, No. 2, Mar-April 2007.
- ¹⁴Williams T., Bolender M. A., Doman D. B., and Morataya O., "Aerothermal Flexible Model Analysis of a Hypersonic Vehicle", AIAA Atmospheric Flight Mechanics Conference and Exhibit, August 2007, AIAA-2007-6395
- ¹⁵Bolender M. A., Oppenheimer M. W., and Doman D. B., "Effects of Unsteady and Viscous Aerodynamics of a Flexible Air-Breathing Hypersonic Vehicle", AIAA Atmospheric Flight Mechanics Conference and Exhibit, August 2007, AIAA-2007-6397
- ¹⁶Rodriguez A. A., Dickeson J. J., Cifdaloz O., McCullen R., Benavides J., Sridharan S., Kelkar A., Vogel J. M., and Soloway D., "Modeling and Control of Scramjet-Powered Hypersonic Vehicles: Challenges, Trends, & Tradeoffs", Guidance Navigation and Control Conference and Exhibit 2009, Honolulu, Hawaii.
- ¹⁷Paus, M., and Well K. H., "Optimal Ascent Guidance for a Hypersonic Vehicle," AIAA Guidance, Navigation and Control Conference, July 1996, San-Diego, CA, AIAA-96-3901.
- ¹⁸Block, R., "The Challenges of Hypersonic Vehicle Guidance, Navigation, and Control", AIAA Space Programs and Technologies Conference Sep 25-28, 1990, Huntsville, AL, AIAA 90-3832.
- ¹⁹Schmidt, D. K., "Integrated Control of Hypersonic Vehicles – A Necessity Not Just a Possibility," AIAA-93-3761-CP.
- ²⁰Schmidt, D. K., "Integrated Control of Hypersonic Vehicles," AIAA/DGLR Fifth International Aerospace Planes and Hypersonics Technologies Conference, Nov-Dec 1993, Munich, Germany, AIAA-93-5091-CP.

- ²¹Gregory, I., McMinn, J., and Shaugnessy, J., "Hypersonic Vehicle Control Law Developments Using H-infinity and Mu-Synthesis", AIAA Fourth International Aerospace Planes Conference, Orlando, FL, 1-4 Dec 1992, AIAA-92-5010.
- ²²Buschek, H., and Calise A. J., "Robust Control of Hypersonic Vehicles Considering Propulsive and Aeroelastic Effects," AIAA-93-3762-CP.
- ²³Lei, Y., Cao, C., Cliff E., Hovakimyan N., and Kurdilla A., "Design of an L1 Adaptive Controller for Air-breathing Hypersonic Vehicle Model in the Presence of Unmodeled Dynamics", Guidance Navigation Control Conference and Exhibit, Aug 2007, Hilton Head, South Carolina, AIAA 2007-6527.
- ²⁴Kuipers, M., Mirmirani, M., Ioannou P., and Huo Y., "Adaptive Controller of an Air-breathing Hypersonic Cruise Vehicle", Guidance Navigation Control Conference and Exhibit, Aug 2007, Hilton Head, South Carolina, AIAA 2007-6326.
- ²⁵Jankovsky, P., Sigthorsson, D. O., Serrani A., Yurkovich S., Bolender M. A., and Doman D. B., "Output Feedback Control and Sensor Placement for a Hypersonic Vehicle Model", Guidance Navigation Control Conference and Exhibit, Aug 2007, Hilton Head, South Carolina, AIAA 2007-6327.
- ²⁶Fiorentini, L., Serrani A., Bolender M. A., and Doman D. B., "Nonlinear Robust/Adaptive Controller for an Air-breathing Hypersonic Vehicle Model", Guidance Navigation Control Conference and Exhibit, Aug 2007, Hilton Head, South Carolina, AIAA 2007-6329.
- ²⁷Gibson T. E., and Annaswamy A., "Adaptive Control of Hypersonic Vehicles in the Presence of Thrust and Actuator Uncertainties", Guidance Navigation and Control Conference and Exhibit 2009, Honolulu, Hawaii.
- ²⁸Levin J., Ioannou P. A., and Mirmirani D., "Adaptive Mode Suppression Scheme for an Aeroelastic Airbreathing Hypersonic Cruise Vehicle", Guidance Navigation and Control Conference and Exhibit 2009, Honolulu, Hawaii.
- ²⁹Kuipers M., Ioannou P. A., Fidan B., and Mirmirani D., "Robust Adaptive Multiple Model Controller Design for an Airbreathing Hypersonic Vehicle Model", Guidance Navigation and Control Conference and Exhibit 2009, Honolulu, Hawaii.
- ³⁰Reiman S. E., Dillon C. H., Lee H. P., and Youssef H. M., "Adaptive Reconfigurable Dynamic Inversion Control for a Hypersonic Cruise Vehicle", Guidance Navigation and Control Conference and Exhibit 2009, Honolulu, Hawaii.
- ³¹Thomson, P. M., Myers, T. T., and Suchomel, C., "Conventional Longitudinal Axis Autopilot Design for a Hypersonic Vehicle," 33rd Aerospace Sciences Meeting and Exhibit, Jan 1995, Reno, NV, AIAA-95-0556.
- ³²Lind R., "Linear Parameter-Varying Modeling and Control of Structural Dynamics with Aerothermoelastic Effects," Journal of Guidance, Control, and Dynamics, Vol. 25, No. 4, July-August 2002.
- ³³Adami T. A., and Zhu J. J., "Control of a Flexible, Hypersonic Scramjet Vehicle Using a Differential Algebraic Approach", Guidance Navigation and Control Conference and Exhibit 2009, Honolulu, Hawaii.

- ³⁴Vaddi S. S., “Guidance and Control of a Moving Mass Actuated Kinetic Warhead using Convex Optimization Techniques”, Guidance Navigation Control Conference and Exhibit 2006, Keystone, Colorado.
- ³⁵Tillerson, M., Inalhan, G., and How J. P., “Co-ordination and Control of Distributed Spacecraft Systems Using Convex Optimization Techniques”, International Journal of Robust and Nonlinear Control, Vol. 12, No. 2, 2002, pp.207-242.
- ³⁶Van Oort E. R., Chu Q. P., Mulder J. A., and Van Den Boom T. J. J., “Robust Model Predictive Control of a Feedback Linearized Nonlinear F-16/MATV Aircraft Model”, Guidance Navigation and Control Conference and Exhibit 2006, Keystone, Colorado.
- ³⁷ Wang Y and Boyd S., “Fast Model Predictive Control Using Online Optimization”, Proceedings of the IFAC World Congress, Seoul, July 2008, pp.6974-6997.
- ³⁸<http://www.stanford.edu/~boyd/cvx/>